Available online at www.sciencedirect.com
SCIENCE DIRECT®
Thin Solid Films 513 (2006) 338–346
thin solid films
www.elsevier.com/locate/tsf

Surface composition gradients of immobilized cell signaling molecules. Epidermal growth factor on gold

Qian Wang, Paul W. Bohn *

Department of Chemistry and Beckman Institute for Advanced Science and Technology, University of Illinois at Urbana-Champaign, 600 S. Mathews Ave., Urbana, IL 61801, USA

Received 11 May 2005; received in revised form 11 January 2006; accepted 11 January 2006
Available online 9 March 2006

Abstract

Surface composition gradients of the signaling molecule, epidermal growth factor (EGF), have been prepared by an adaptation of the electrochemical gradient technique. EGF is covalently bound to the reactive component, 11-amino-l-undecanethiol (AUT), in a counter-propagating two-component gradient composed of AUT and poly(ethylene glycol) thiol (PEG) using carbodiimide coupling chemistry. Areas of the surface presenting $-NH_2$ termination react with succinimidyl esters of solvent-accessible acidic amino acids in EGF, while non-specific protein adsorption is resisted in the PEG regions. The maximum surface coverage of EGF prepared in this manner was determined by surface plasmon resonance reflectometry (SPR) on spatially uniform films to be $20\% < \Gamma_{EGF} < 70\%$ depending on the concentration of the EGF derivatization solution. EGF retains its biological activity with this immobilization process, as verified by culturing human umbilical vein endothelial cell (HUVEC) on an EGF-terminated surface for 24 h. PEG shows good resistance to EGF physical adsorption as demonstrated by both SPR and X-ray photoelectron spectroscopy (XPS). The N/C ratio of EGF gradients, which is characteristic of EGF adsorption, because only the protein contains N, while both protein and PEG contain C, was spatially mapped with XPS. The gradient composition distributions are sigmoidal with lateral distance, with the position of the gradient transition region being readily controlled by adjusting the applied potential window. EGF gradients with variable quantitative surface coverage profiles were generated by varying EGF and AUT concentrations.

Keywords: Gradient; Epidermal growth factor; X-ray photoelectron spectroscopy; Gold

1. Introduction

Cell migration is crucial in embryonic development, the inflammatory immune reponse, wound repair, tumor formation and metastasis [1]. Understanding the fundamental mechanisms underlying cell migration is the key to developing more effective therapeutic approaches for treating disease, approaches to cellular transplants, and the preparation of artificial tissues [2]. Epidermal growth factor (EGF) is small (MW 6100 Da), heat stable [3] and capable of inducing both mitogenic and motogenic responses in cell types such as fibroblasts, epithelial cells, and keratinocytes. The signaling pathways controlled by the EGF family of growth factors and their receptors are capable of regulating the proliferation and differentiation of many tissue types [4,5]. Uncontrolled activation of these pathways has been implicated in a number of human cancers including those of the brain, lung, breast, ovary, pancreas and prostate. Increased levels of the epidermal growth factor receptor (EGFR), a receptor for EGF and related ligands, are noted in cancers in correlation with tumor progression to the invasive and metastatic state [6]. It has been suggested that increased EGFR expression leads to increased EGFR-mediated cell motility and proliferation, two factors required for tumor progression. In addition, EGF-dependent increases in cell proliferation and motility have been implicated in accelerated wound healing. Thus, the binding of extracellular EGF to its receptor and its ability to mediate cell motility has important pathological and physiological ramifications.

Uniform concentrations of EGF induce chemokinesis, while EGF gradients induce chemotaxis [7–9]. Soon et al. [10] have shown that EGF gradients generated with a micropipette

* Corresponding author. Tel.: +1 217 333 0676; fax: +1 217 244 8068.
E-mail address: bohn@scs.uiuc.edu (P.W. Bohn).

0040-6090/$ - see front matter © 2006 Elsevier B.V. All rights reserved.
doi:10.1016/j.tsf.2006.01.067

specifically induced polarized morphology and chemotaxis of metastatic mammary tumor cells. Wang et al. [11] have developed EGF gradients in a microfluidic chemotaxis chambers and reported MDA-MB-231 cancer cell chemotaxis that depends on the shape of the EGF gradient profile as well as on the range of EGF concentrations. Extensive previous work on EGF-induced chemotaxis makes it an ideal system to study the molecular mechanisms involved in cancer cell chemotaxis and their relation to metastasis. There are also important differences in cellular response to immobilized vs. soluble EGF. It has been demonstrated that immobilized growth factor proteins not only regulate cell functions without being internalized, but also enhance intracellular signaling [12–14]. The measured activity of immobilized EGF is higher than the soluble form, possibly because immobilization inhibits the down-regulation induced by ligand internalization. For example, Griffith and Kuhl reported that EGF tethered on aminosilane-modified glass via star poly (ethylene oxide) retains its biological activity and is as effective as soluble EGF in eliciting DNA synthesis and cell rounding responses in primary rat hepatocytes [3]. Ito [14] immobilized EGF on a surface-hydrolyzed poly(methyl methacrylate) film and found that immobilized growth factor can regulate cell functions without cellular internalization. In addition, cell growth was significantly enhanced on the immobilized-EGF film, the enhancement being larger than that obtained with diffusible EGF. The effects of EGF and the extracellular matrix protein fibronectin (FN) on multiple facets of fibroblast motility have been reported [4], so access to stable, quantitatively characterized EGF gradients with controlled surface characteristics would be a significant boon to cell chemotaxis studies. However, most previous studies address the influence of spatially uniform distributions of signaling molecule EGF on cell-substratum interactions, and there has not been, up to now, a reliable and general method to produce spatially controlled distributions of immobilized EGF on surfaces.

Creating well-defined gradients in surface composition has proven to be a substantial experimental challenge. Several methods have been demonstrated that use self-assembled monolayers (SAMs) to generate gradients in surface properties, including photoimmobilization of peptides on SAMs [15] and reaction–cross diffusion [16,17]. For example, *R*-phycoerythrin gradients have been created using a heterobifunctional photolinking agent with varying exposure time to laser irradiation [18]. Also, microfluidics have been used to generate surface and solution gradients of laminin in order to study neuronal growth [19,20]. A new technique to make surface composition gradients on thin Au electrodes, which exploits the electrosorption properties of alkanethiols, has been developed in our laboratory [21–25]. Adsorbed thiols on Au, RS–Au, are electrochemically stripped from Au surfaces by reductive desorption, which results in the release of RS^- [26–29]. By coupling the thiol stripping reaction to a non-uniform in-plane electrochemical potential distribution, $V(x)$, thiols can be stripped from regions of the surface where the local potential favors desorption. The resulting gradient in surface potential produces a surface composition profile, $\Gamma(x)$, which progresses from bare Au on one end to any desired level of thiol coverage at the other end. The bare regions can then be back-filled with another thiol, creating a two-component full monolayer. Changing the terminal group, therefore, allows two-component systems with spatially graded chemical and physical properties to be fabricated. The spatial position of the transition region between the two components depends on the value of the desorption potential, E^0_{des}, for the first thiol. Since the electrochemical strategy for creating two-component gradient structures is largely independent of the ω-functional group of the thiol, molecular recognition motifs may be inserted at the solution-accessible end of the thiol molecule to produce well-defined spatial gradients of molecular recognition moieties.

Because the details of cellular motility depend on the spatial rate of change of growth factor, $\mathrm{d}\Gamma/\mathrm{d}x$, it is important to characterize the spatial variation in the transition region in order to understand the range and spatial dispersion of the in-plane growth factor composition distributions. Various approaches have been taken to characterizing biologically active surface composition gradients. Fourier Transform Infrared External Reflection Spectroscopy (FTIR-ERS) [30] and Matrix-Assisted Laser Desorption/Ionization Mass Spectrometry (MALDI-MS) [31] have been used to map spatially controlled RGD (arginine–glycine–aspartic acid) peptide gradients. Gradients of the extracellular matrix protein FN, produced by covalently binding FN on two-component thiol gradients with selective amine chemistry, present a more significant challenge, primarily due to the much higher molecular weight and plethora of structural motifs. However, composition profiles of FN gradients have been characterized in our laboratory by a sandwich antibody assay in which anti-FN recognizes surface-bound FN and the spatial distribution of fluorescently labeled IgG is imaged by fluorescence microscopy [32].

In this paper, we used similar amine chemistry to develop spatially controlled EGF gradients with various surface densities. Initially a two-component gradient consisting of 11-amino-1-undecanethiol (AUT) and poly(ethylene glycol) thiol (PEG) is created. EGF is then mapped onto this small-molecule gradient by reaction of the terminal amino functionality with NHS (*N*-hydroxysuccinimide)-activated esters of EGF. Reaction progress is monitored with surface plasmon resonance (SPR) reflectometry, and the presence of a gradient in surface-immobilized EGF is confirmed by X-ray photoelectron spectroscopy (XPS) by mapping the surface N/C ratio, characteristic of the presence of EGF.

2. Experimental details

2.1. Materials

11-amino-1-undecanethiol hydrochloride was purchased from Dojindo Molecular Technologies. PEG, MW 2000, was purchased from Shearwater Corporation. Human EGF, NHS) and 1-ethyl-3-(3-dimethylaminopropyl) carbodiimide (EDC) were received from Sigma. KOH and NaOH were purchased from Fisher Scientific. Absolute ethanol (EtOH) was purchased from Aaper Alcohol and Chemical. All reagents were used as received.

2.2. Substrate preparation

BK-7 microscope slides were used as substrates for Au deposition. Prior to metal deposition, slides were cut into 15 × 10 mm pieces and cleaned in a freshly prepared Piranha (4 : 1 H_2SO_4 : H_2O_2; *Caution: Piranha is a vigorous oxidant and should be used with extreme caution*!) solution, rinsed thoroughly with doubly deionized H_2O and 2-propanol and blown dry with N_2. The samples were then immediately transferred to the evaporation chamber. Chromium (1 nm) was evaporated to promote adhesion of Au on glass, followed by evaporation of 50 nm of Au for glass and 47 nm for SF10 prism. Au films were vapor deposited on the slides as 15 × 3 mm rectangles for XPS measurement. Samples were stored under N_2 until ready for use. Samples were then immersed in a 1 mM ethanolic solution of thiol for at least 1 h, rinsed with EtOH and dried with N_2. Substrates for surface plasmon resonance measurements were prepared by evaporating 47 nm of Au with a 1 nm Cr layer directly on a SF-10 prism.

2.3. EGF immobilization

Forty micrograms per milliliter of EGF in 10 mM phosphate buffer (pH 6.0) was mixed with a freshly prepared aqueous solution of 75 mM EDC and 15 mM NHS and gently stirred for 15 min. Au films supporting AUT SAMs or AUT-PEG gradients were then immersed in the EGF-NHS solution for 1 h. The samples were rinsed with water and placed in a Petri dish in 0.1 M NaOH on an orbital shaker at speed of 100 rpm for 1 h in order to remove non-specific adsorption of EGF, replacing NaOH solution each 10 min. Samples were then removed from the solution, rinsed with water, and blown dry with N_2.

2.4. Gradient formation

Au films were soaked in 1 mM ethanolic AUT for at least 1 h, rinsed with EtOH and dried with N_2. A bipotentiostat (Pine Instruments model AFCBP1) employing a Ag/AgCl reference electrode and a Pt mesh counter electrode was used to apply the desired electrochemical potentials to the two ends of the working electrode in 0.25 M KOH/MeOH supporting electrolyte. The potential window width, ΔV, and the center value of the potential, V_0, were used to characterize the applied potential window. Potential was applied for 5 min to achieve one-component gradients in AUT. After electrolysis, samples were quickly removed from the electrolyte solution, rinsed with EtOH and immediately immersed in a 1 mM aqueous solution of PEG thiol for 3 min. Then the sample was rinsed with water and dried with N_2. Samples were stored in water until ready to use, generally within an hour.

2.5. Surface plasmon resonance measurements

A 650 nm linearly polarized, single mode diode laser with an output of approximately 4 mW was spatially filtered and adjusted to p-polarization. A cylindrical lens focused the radiation to a line on a 47 nm thick Au film on a SF10 prism in the Kretschmann configuration. The diverging reflected beam was collimated, and the angular dispersion of reflected light intensity was mapped across a CCD detector array. SPR data were collected on a Photometrics PM512 CCD camera using Photometrics CCD 9000 software. The intensity profiles were fit to a polynomial from which the angle of minimum reflectance was extracted. The active Au surface was contained in a Teflon flow cell that allowed introduction of reagents and real time monitoring of the surface reactions. A Masterflex (Cole–Parmer) variable speed pump with a flow rate range of 0.5–10 mL/min controlled solution flow rate through the cell.

2.6. X-ray photoelectron spectroscopy (XPS)

XPS data for EGF gradients were collected using a Kratos AXIS ULREA spectrometer with monochromatic Al Kα radiation at 1486.6 eV (225 W). Scans were obtained at pass energy of 160 eV for survey scans and 40 eV for high-resolution scans. The pressure in the spectrometer was typically 10^{-9} Torr. Samples were held on a rectangular metal support by copper contact tape, and an area ca. 0.3 × 0.7 mm was probed. Once the samples were introduced into the sample analysis chamber, they were manipulated in the x, y and z directions and monitored by a CCD camera. Spatial measurements were referenced to the 15 × 3 mm Au films. Eight equally separated spots along the 15 mm long active gradient region were chosen for XPS characterization. Each gradient profile shown in Results and Discussion represents one single measurement for one gradient. The XPS signal error was not measured for each gradient due to short of material and time. All samples were analyzed at a 90° angle relative to the sample surface with the neutralizer on. After subtraction of a linear background, all spectra were fit using Voigt profile (70% Gaussian–30% Lorentzian) peaks, taking the minimum number of peaks consistent with the best fit.

2.7. Cell culture and adhesion assay

Human umbilical vein endothelial cells (HUVEC) were cultured in Dulbecco's modified Eagle's Medium (DMEM) supplemented with 5% fetal bovine serum (FBS). For adhesion assays, cells were detached by trypsinization, the trypsin was stopped by addition of medium with trypsin inhibitor, and cells were pelleted by low-speed centrifugation and resuspended in medium containing 5% FBS. Cell suspensions (3×10^5 cells/mL) were added in a microfluidic device with a 400 μm wide × 400 μm deep channel overlaying EGF adsorbed on Au. Cell images were taken after 24 h incubation.

3. Results and discussion

3.1. EGF immobilization

First, an activated ester of EGF is produced by carbodiimide coupling to the solvent-accessible carboxylic acid moieties on the oligopeptide. In a separate step an amino-terminated lateral gradient of AUT is formed by coupling reductive desorption of AUT to a spatial gradient of the electrochemical potential, as

shown in Scheme 1. Subsequently the EGF-ester is reacted with the amine terminal functionalities of the AUT SAM on Au to transfer the initially formed AUT gradient into a spatial gradient of EGF. In this strategy, the areas not supporting reactive amine functionalities can induce nonspecific-adsorption of EGF, degrading the original EGF spatial gradient. Ideally the second component of the two-component counterpropagating gradient should resist EGF physisorption and be unreactive under the conditions used for EGF immobilization. Since peptides and proteins adsorb readily onto bare Au [33], PEG is used as the second, protein adhesion-resistant, component [34,35]. In order to remove any remaining unreacted EGF from the surface after covalent immobilization, the gradient substrates are immersed in 0.1 M NaOH and gently shaken. The strongly basic pH (pH > 12) has two mutually reinforcing effects. It enhances hydrolysis of unreacted succinimidyl esters, and the large ionic strength reduces electrostatic interactions between physisorbed EGF and the sample surface.

The amine chemistry used to immobilize EGF on an AUT spatial composition gradient exploits the fact that EGF contains many exposed and reactive carboxylic groups. Thus, although the reactions scheme shown in Scheme 1 implies that EGF is modified with a single activated ester, in fact, the number of activated esters per EGF molecule is undefined and likely more than one. In the pH range $4 < pH < 8$ the normalized surface coverage is $\Gamma_{EGF} = 22 \pm 6\%$ independent of pH, indicating that pH does not exert significant influence on the EGF assembly reaction near neutral pH. Increasing the concentration of the EGF coating solution from 40 to 80 μg/mL results in an increase of the EGF surface coverage of ca. a factor of 3. We did not test derivatization solutions more concentrated than 80 μg/mL due to cost constraints, however, the increase in surface coverage is probably associated with multilayer formation, since the active ester of EGF can react with other EGF molecules, as well as the surface-immobilized AUT. We also tried to use the substrate-active succinimide chemistry [32] in order to generate EGF monolayer gradients, but EGF chemisorption was negligible in this approach, presumably because there are only two free amine groups in EGF, resulting in very low binding efficiency. In cell chemotaxis studies, it is not critical to control multilayer coverage of EGF as long as EGF remains biologically active on the surface. In order to verify the biological activity of EGF, HUVEC were plated onto PEG, FN and EGF + FN uniform samples. Fig. 1 shows cell adhesion images on the three samples after 24 h incubation. The cells are round and dead on PEG, indicating that PEG inhibits cell adhesion very efficiently. The cells placed on FN adhere and spread well, however the amount of cell adhesion increases significantly when EGF is added 1 : 1 to FN. This indicates that EGF retains its active conformation and stimulates cell proliferation on the surface resulting in much more cell attachment on EGF + FN than on FN. The biologically active, varied surface density EGF gradients described here should, therefore, be useful in the future for delineating more subtle aspects of EGF-stimulated signaling behavior.

In order to characterize the covalently immobilized EGF layer quantitatively, SPR reflectometry was used to monitor the

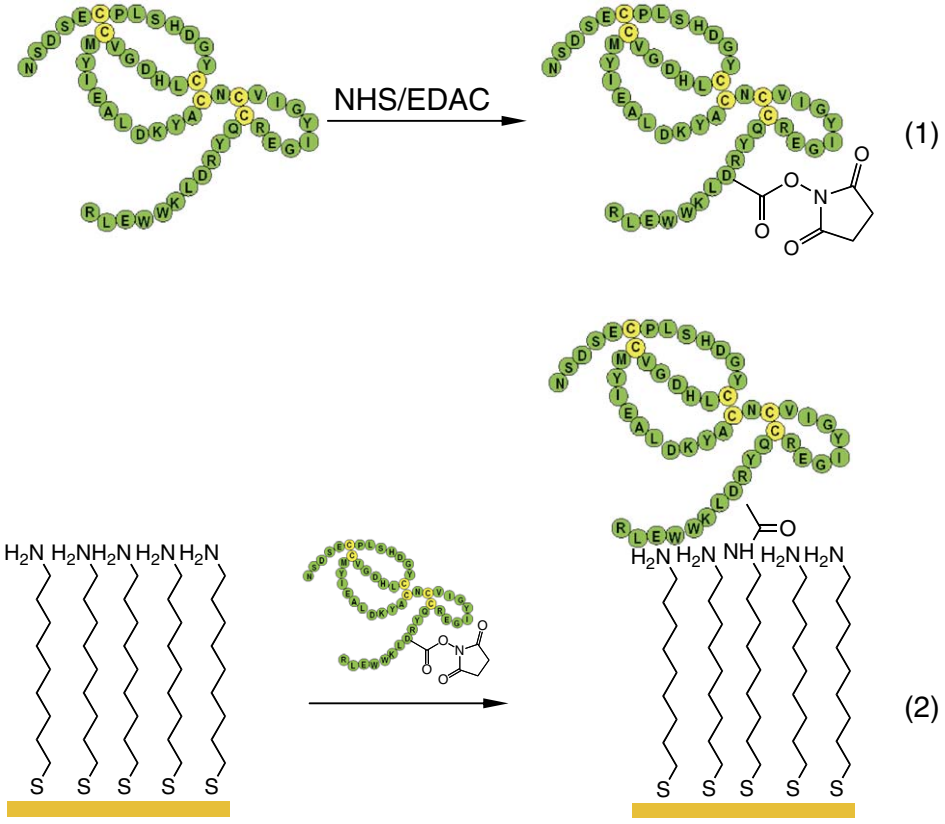

Scheme 1. Immobilization chemistry of EGF.

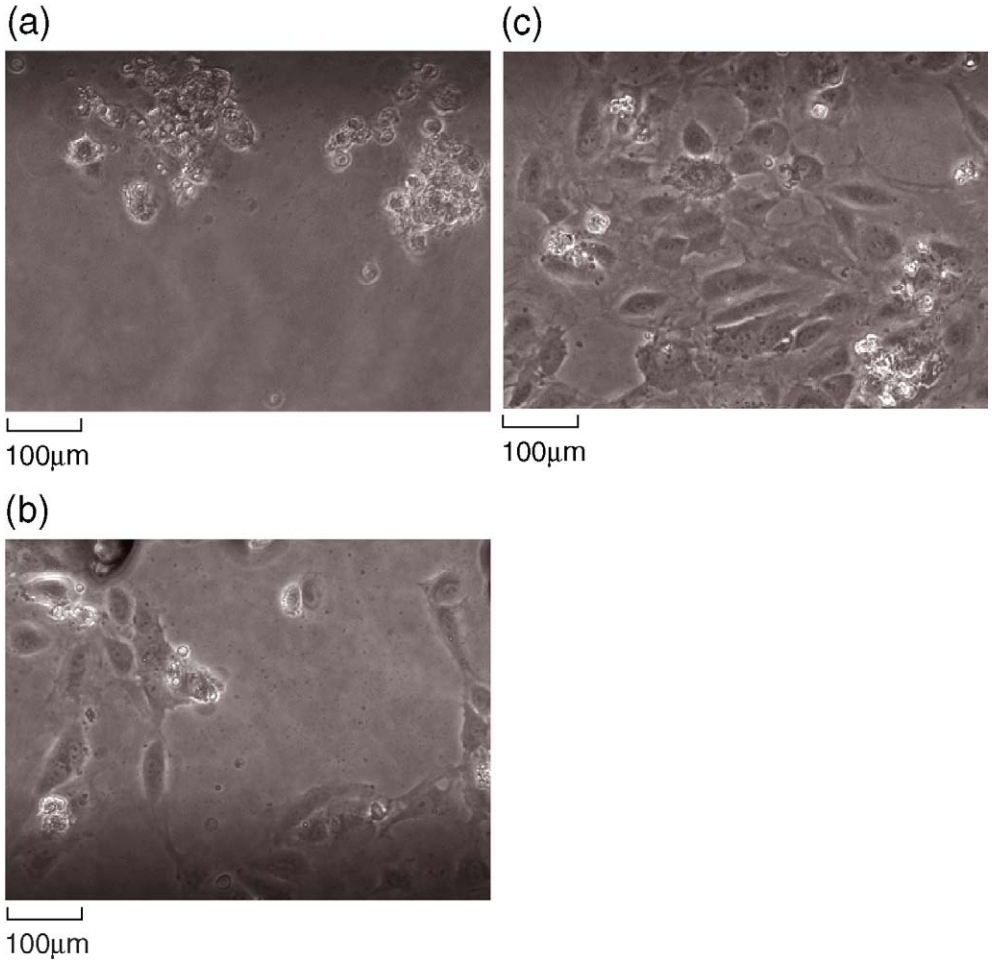

Fig. 1. Optical microscope images showing the adhesion of HUVEC on PEG (a), FN (b) and EGF+FN (c) assembled on Au surface after 24 h cell culture. EGF+ FN represents 1 : 1 EGF : FN during immobilization process.

immobilization of EGF. The surface plasmon resonance of a thin Au film is signaled by a minimum in the reflected light intensity in the Kretschmann configuration and is very sensitive to the dielectric response function, $\varepsilon(k,\omega)$, of the metal–liquid interface [36,37]. The assembly of submonolayer films at the Au–electrolyte interface can be monitored in situ in real time by following the angle of minimum reflectance, θ_{min}, as a function of time. Since the position of the resonance minimum can be calculated from the Fresnel relations and depends on the dielectric constant of all optical films in the stratified medium, as well as the thickness of the surface layers [38], this provides a powerful means of following the development of the EGF surface adlayer.

Fig. 2 shows the measured shift in θ_{min} as a function of time for the immobilization of EGF and tagging reagents on AUT and PEG. In order to monitor $\Delta\theta_{min}$ from one reagent to another, θ_{min} must be compared during exposure to the same solvent (H_2O), to correct for the non-negligible change in bulk refractive index among different solvents and solutions. After reacting the AUT monolayer with EGF active ester, an initial shift of 0.22° is observed (between point b and the baseline in Fig. 2). Exposure of the PEG monolayer to the same active EGF

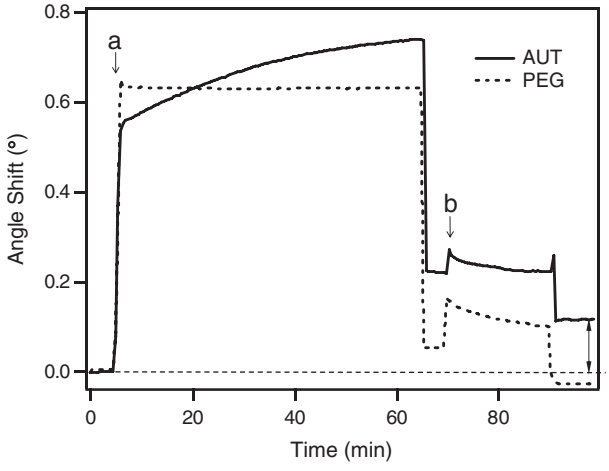

Fig. 2. SPR resonance position as a function of reagent exposure/rinsing steps during EGF assembly on AUT and PEG. Arrows indicate the introduction of reagents: (a) NHS, EDC and 40 μg/mL EGF, and (b) 0.1 M NaOH. Rinse cycles with water were performed at the beginning, between reagent additions and at the end. The baseline (dashed line) indicates the original position of θ_{min}, and the double arrow indicates the shift in θ_{min} associated with EGF adlayer formation on the AUT surface.

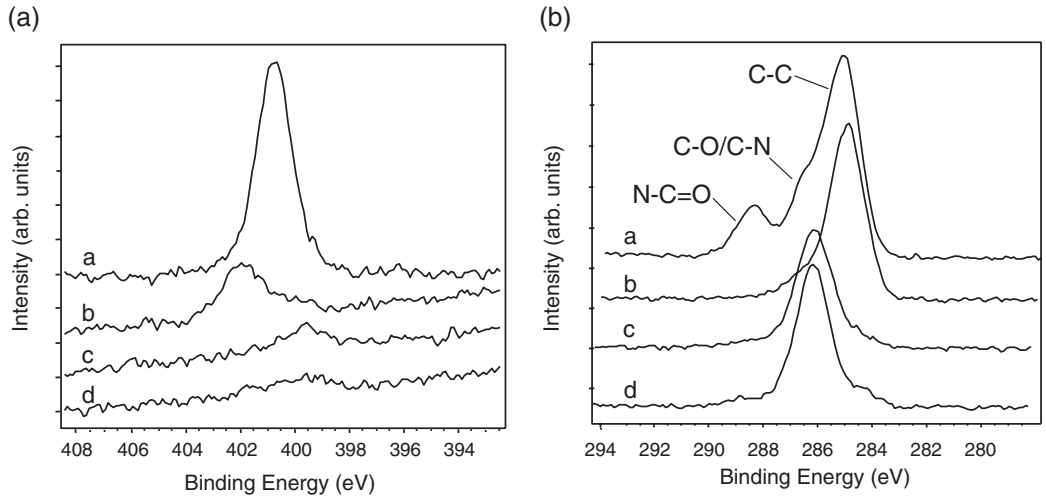

Fig. 3. XPS spectra from EGF-AUT (curve a), AUT (curve b), EGF-PEG (curve c) and PEG (curve d) surfaces in the N_{1s} (a) and C_{1s} (b) regions of the XPS spectra.

ester reagents results in a net shift of 0.05°. It is obvious a larger angular shift is observed on AUT than on PEG during EGF assembly. Rinsing with base results in EGF loss, corresponding to the removal of physisorbed EGF, from both monolayers as well as the hydrolysis of any remaining succinimidyl esters. The result is a net shift of 0.11° on AUT and ~0° on PEG. Clearly under these conditions PEG exhibits excellent biological inertness and resistance to non-specific adsorption of EGF.

The coverage of EGF can be recovered by quantitative modeling of the SPR resonance shift data [32]. Briefly, the optical response function of the five-layer system, composed of prism, Au film, thiol monolayer, EGF layer and water, is modeled. In the fitting procedure, the thickness and dielectric constants of the prism, Au film, thiol layer and water are held constant, and the composition of the EGF layer, i.e. the dielectric response, is allowed to vary. The effective dielectric constant of the EGF layer is calculated from the measured angular shift in θ_{min}, assuming a thickness equal to a hypothetical full monolayer of EGF. Effective medium theory is then used to determine the fractional coverage of EGF, taking the dielectric constants and thickness for AUT as $\varepsilon_{AUT}=2.10$ and $d_{AUT}=1.6$ nm [39,40], and those for EGF as $\varepsilon_{EGF}=2.25$ and $d_{EGF}=2.2$ nm [41]. In the assembly sequences shown in Fig. 2, the final net shift $\Delta\theta_{AUT}=0.11°$ for EGF immobilization corresponds to an EGF fractional coverage, $\Gamma_{EGF}=23\%$, whereas Γ_{EGF} ~0 on the PEG surface consistent with the negligible angular shift. When the concentration of the EGF coating solution increases from 40 to 80 μg/mL, the average EGF coverage increases from 23% to 72%.

3.2. Characterization of EGF assembly

Fig. 3 shows high-resolution XPS scans in the N_{1s} (a) and C_{1s} (b) regions from AUT and PEG SAMs before and after EGF immobilization. The presence of N is an excellent indicator specific to adsorbed protein [42,43], because its presence is typically unaffected by surface contamination during sample preparation and handling. The base-specific N/C ratio reflects the presence of adsorbed EGF and can be used to characterize EGF assembly on AUT and PEG. The most intense N_{1s} peak at 400.0–401.1 eV in Fig. 3(a) appears following EGF immobilization on AUT. The N_{1s} peak from the AUT SAM is only 32% as intense as that from EGF on AUT. The AUT N_{1s} signal is also clearly distinguished from the EGF-AUT N_{1s} signal by its higher binding energy, consistent with the more electron-withdrawing environment of the amide N atoms which dominate the EGF signal, compared to the primary amine N atoms in AUT. Although the number of N atoms on the EGF-derivatized surface is expected to be far greater than the ca. 3:1 intensity ratio observed, the depth-dependent signal generation mechanism in XPS moderates the intensity of sub-surface N atoms with an exponential sub-surface depth falloff. Immobilizing EGF on PEG produces a very weak (2% of the AUT-EGF N_{1s} peak intensity) N_{1s} peak, likely due to remaining physisorbed EGF not removed by the base rinse. Again this very low level N_{1s} signal is consistent with highly protein adhesion-resistant behavior of PEG.

Satisfactory fits of the C_{1s} peak of EGF on AUT in Fig. 3(b) require three components at binding energies of 285.0, 286.4 and 288.3 eV, corresponding to hydrocarbon, the more electronegative C–N and C–O species, and N–C=O functionalities, respectively. Table 1 shows the relative intensity ratios of the three components in AUT and PEG before and after EGF assembly. Several features of the quantitative peak fitting are noteworthy. First, as expected from qualitative inspection of the spectra, the EGF-AUT sample has the largest N/C ratio,

Table 1
Relative XPS N_{1s} and C_{1s} elemental signals

Sample	Hydrocarbon (%)	C–N/C–O (%)	N–C=O (%)	N/C
AUT	88	12	0	0.09
AUT-EGF	63	21	16	0.19
PEG	8	92	0	0.03
PEG-EGF	6	93	1	0.05

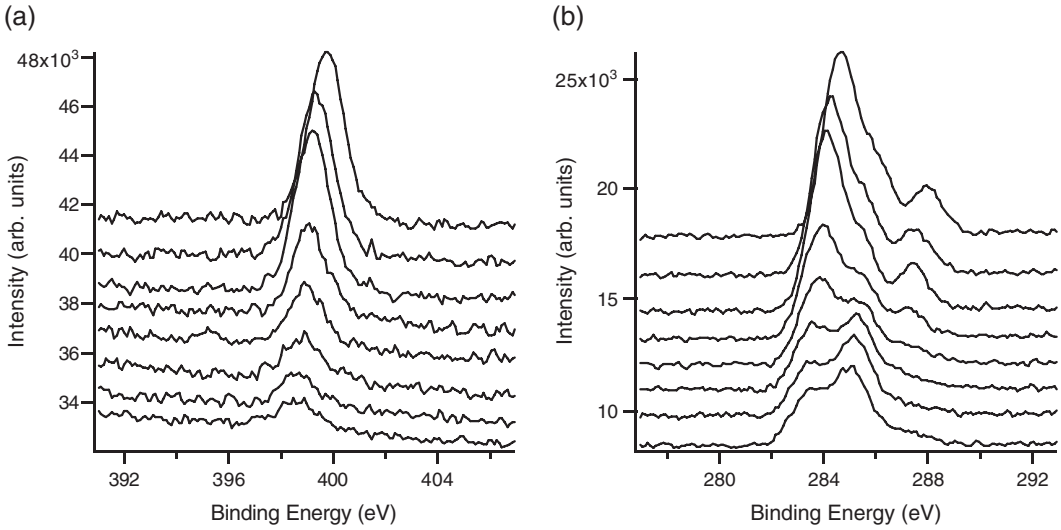

Fig. 4. (a) XPS N_{1s} spectra and (b) XPS C_{1s} spectra from an EGF/PEG gradient produced with applied potential window $-0.3\,V > \Delta V > -1.3\,V$ (vs. Ag/AgCl). In both sets of spectra the eight curves from down to up represent spectra from full PEG to full EGF coverage end with 1.5 mm distance.

consistent with the immobilization of the EGF peptide [44]. AUT itself has an intermediate value, and the PEG samples have small values. Furthermore, in the AUT SAM most carbon is present as hydrocarbon with 12% of the C_{1s} peak at 286.4 eV being from the terminal C–NH_2 group. After EGF immobilization, a C_{1s} peak appears at 288.3 eV, corresponding to the N–C=O group. This is the highest binding energy peak in any of the C_{1s} spectra, consistent with the carbonyl carbon being bonded to the strongly electronegative O atom. Finally, assembly of EGF on PEG surfaces produces XPS spectra at both the C_{1s} and N_{1s} energies which are indistinguishable from the underivatized PEG surface.

3.3. Gradient formation and characterization

EGF gradients are produced by first forming a AUT gradient, then backfilling with PEG to produce a two-component counter-propagating thiol gradient. Subsequently, EGF is immobilized on the AUT/PEG gradient by reaction of the active ester with the gradient terminal amines on the AUT. The two-component gradients are characterized by XPS spatial mapping. Fig. 4 shows a series of spatially resolved XPS spectra of N_{1s}, Fig. 4(a), and C_{1s}, Fig. 4(b), peaks acquired from 8 equally spaced positions along the 15mm long active transition region of a EGF/PEG gradient film on Au. It is clear that the N_{1s} peak intensity in Fig. 4(a) increases as the potential shifts positively, i.e. as the position shifts from 1.5 mm to 12.0 mm. As noted previously a small peak is observed at the fully PEG-covered end due to remaining physisorbed EGF. The C1s spatial mapping data also show trends consistent with observations from the single component spectra in Fig. 3. Proceeding along the gradient from the PEG to the EGF end the 285.0 eV (C–N/C–O) and 288.3 eV (N–C=O) peaks increase. Both N_{1s} and C1s spectra are consistent with the existence of a spatial composition gradient in the surface density of the signaling ligand EGF.

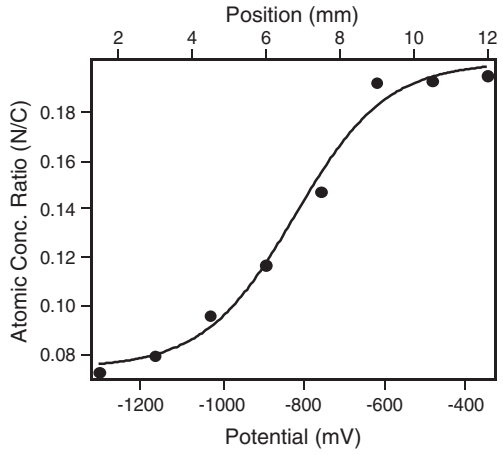

Fig. 5. N/C atomic concentration ratio for a specific EGF/PEG gradient as a function of applied potential (bottom abscissa) and spatial position (top abscissa). Solid line is a fit to Eq. (1).

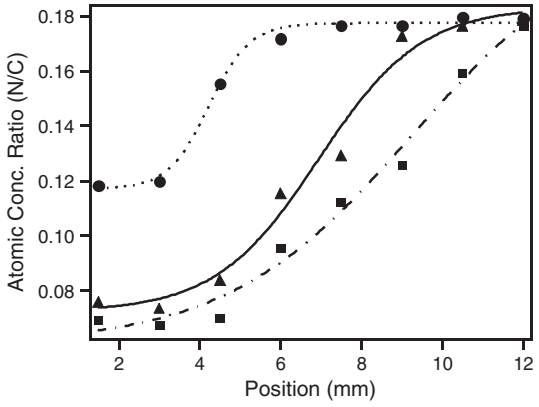

Fig. 6. N/C atomic concentration ratio as a function of spatial position for three EGF/PEG gradients prepared with potential windows of variable center potential, but constant width, ΔV. (—●—) $-0.3\,V > \Delta V > -1.1\,V$; (–▲–) $-0.45\,V > \Delta V > -1.25\,V$; (-·-■-·-) $-0.6\,V > \Delta V > -1.4\,V$. In each case the lines are fits to Eq. (1).

The N/C ratio can also be used to map the spatial composition profiles of EGF/PEG gradients, since it reflects the presence of adsorbed EGF, but not PEG. Fig. 5 shows a plot of N/C ratio as a function of applied potential or, equivalently, lateral position along the Au film, x, fitted to a sigmoidal function of the form,

$$F(x) = F_b + \frac{F_{max}}{1 + e^{(x_0 - x)/r}} \quad (1)$$

where F_b is an offset, F_{max} is the normalized maximum fraction, x_0 is the inflection point of the slope region, and r is a spatial rate constant related to the slope of the gradient. The fitting function is especially useful as a mechanism to extract parameters, such as the center of the transition region, x_0, and the width, W, determined from the full width at half-maximum of the derivative of the fit function, $F(x)$. The x_0 and W values can be converted between potential space and physical space using the magnitude of the applied potential window, ΔV, and the total length of the film. Comparison in potential space is especially useful, inasmuch as it allows different gradients to be compared on a common footing.

The gradient formation characteristics are determined by the distribution of the local electrochemical potential, $V(x)$. By shifting the potential window, ΔV, experimentally one can learn how the gradient formation characteristics change as the local potential, $V(x)$, is moved relative to the physical frame of the active region. This can be seen clearly in the data for the three gradients shown in Fig. 6. By keeping ΔV constant and moving the center potential, V_0, negatively, it is apparent that the transition region shifts in physical space, i.e. to the right in Fig. 6. The fits to Eq. (1) summarized in Table 2 also indicate that the gradient center in physical space shifts significantly to the right, consistent with the predictions of the quasi-linear potential gradient model [14], but remain relatively constant in potential space. The gradient width also changes as the center position of the applied potential window is moved in potential space, but this relationship is more difficult to interpret due to subtle kinetic effects as seen previously in small molecule gradients [17].

One of the great virtues of the electrochemical gradient approach is that, by careful adjustment of the reaction conditions, the endpoint compositions, Γ_{left} and Γ_{right}, can be made to arbitrary specifications, not just 0 and 1. The coverage of EGF within the gradient may be tuned by adjusting the EGF solution concentration and the AUT surface density, Γ_{AUT}. Fig. 7 shows the N/C ratio as a function of spatial position for gradients prepared with different EGF and AUT concentrations. Decreasing the AUT composition, from 100% AUT to 50% AUT + 50% PEG, in the SAM prior to reductive desorption with the same EGF immobilization solution concentration, 40 μg/mL, results in a decrease in the N/C ratio by approximately a factor of 2, a reasonable value given that EGF can access only half the number of $-NH_2$ binding sites for assembly on 50% AUT. When EGF solution concentration increases from 40 to 80 μg/mL, a 20% increase in EGF coverage is observed, consistent with the SPR results on spatially uniform films. Although SPR showed much larger increases in EGF surface loading at 80 μg/mL, the N/C ratio derived from XPS measurements, and used to map EGF spatial distributions, is relatively insensitive to multilayers, as discussed previously. The ability to control the spatial rate of change of the ligand density is a critical requirement for the use of these biomaterials in cell motility studies, and the studies shown in Fig. 7 illustrate the ability to adjust the endpoint compositions as well as the spatial rate of change, $d\Gamma/dx$.

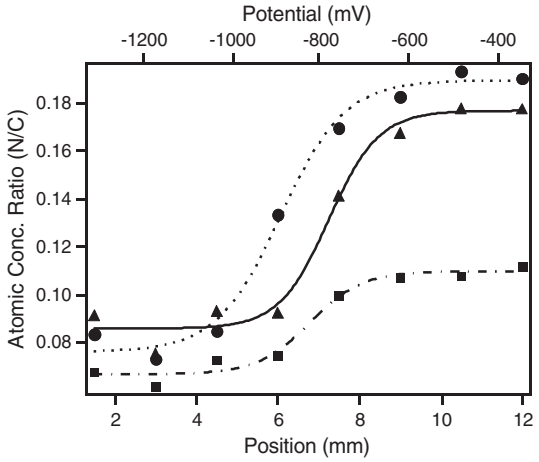

Fig. 7. N/C atomic concentration ratio as a function of gradient position of EGF/PEG gradients with varying concentrations of AUT and EGF in the derivatization solutions. (—●—) 80 μg/mL EGF + 100% AUT; (–▲–) 40 μg/mL EGF + 100% AUT; (-·-■-·-) 40 μg/mL EGF + 50% AUT. In each case the lines are fits to Eq. (1).

4. Conclusions

The spatiotemporal control of surface composition afforded by the in-plane control of electrochemical potential distributions is extended to the creation of surfaces having a well-defined gradient in the surface concentration of the covalently immobilized signaling molecule, EGF. An effective strategy starts by creating a counterpropagating two-component gradient from precursor organothiols, one of which terminates with a primary amine group that can react with activated esters formed from pendant carboxyl groups on the protein. The other

Table 2
Gradient center positions in potential and physical space

Applied potential window (mV)	Applied potential range (mV)	Applied potential window center (mV)	Gradient center (mV)	Gradient center (mm)
−0.30 > V > −1.10	0.80	−0.70	−0.90	4.2
−0.45 > V > −1.25	0.80	−0.85	−0.85	6.9
−0.60 > V > −1.40	0.80	−1.00	−0.83	9.3

component, PEG, is chosen to be unreactive toward EGF immobilization and to be inherently resistant to non-specific adsorption of proteins. The reaction produces a gradient in EGF coverage with maximum coverages in the range 20% $<\Gamma_{max}<$70% determined by the concentration of the EGF immobilization solution. At the higher concentrations the immobilized EGF is almost certainly present as a multilayer, because EGF activated esters can react with pendant amine groups on other EGF molecules as well as surface AUT. Spatial composition profiles can be mapped by XPS, by exploiting the lack of N atoms in the PEG protein adhesion-resistant component, and are well-described by a sigmoidal function. Fits to the sigmoidal function yield the position of the gradient center, which is found to shift in physical space, but not in potential space. The spatial position of the transition region can be readily controlled through the position of the applied potential window in physical space, consistent with the quasi-linear potential gradient model. The fractional coverage of EGF on gradient structures may also be tuned by controlling the areal density of reactive esters derived from AUT. This capability is crucial, because it is critical to control the spatial rate of change of the protein density for quantitative studies of cell adhesion and motility.

The achievement of tunable composition gradients of signaling molecules, such as EGF, has important implications for the study of cellular motility and haptotactic behavior. Now it should be possible to combine gradients of signaling ligands with independently controlled gradients of cell adhesion/motility effectors. The process by which the gradient is formed is not specific to EGF, requiring only the presence of solvent-accessible primary amines, thus lending itself readily to the immobilization of a variety of other biological molecules of interest. The ability to evaluate such protein gradients accurately will enable the study of complex protein distributions and their effect on cellular haptotaxis.

Acknowledgements

This work was supported by the National Institutes of Health (NIGMS GC10825, the Cell Migration Consortium, and NS31609). Film characterization was carried out in the Center for Microanalysis of Materials in University of Illinois supported by the U.S. Department of Energy under grant DEFG02-ER45439. The authors thank Rick Haasch for his assistance with XPS measurements and Thomas E. Eurell for his advice with cell culture experiments.

References

[1] A.F. Horwitz, Sci. Am. 276 (1997) 46.
[2] A.J. Ridley, M.A. Schwartz, K. Burridge, R.A. Firtel, M.H. Ginsberg, G. Borisy, J.T. Parsons, A.R. Horwitz, Science 302 (2003) 1704.
[3] P.R. Kuhl, L.G. Griffith, Nat. Med. 2 (1996) 1022.
[4] I. Alroy, Y. Yarden, FEBS Lett. 410 (1997) 83.
[5] D.J. Riese, D.F. Stern, Bioessays 20 (1998) 41.
[6] G. Maheshwari, A. Wells, L.G. Griffith, D.A. Lauffenburger, Biophys. J. 76 (1999) 2814.
[7] C. Sawyer, J. Sturge, D.C. Bennett, M.J. O'Hare, W.E. Allen, J. Bain, G.E. Jones, B. Vanhaesebroeck, Cancer Res. 63 (2003) 1667.
[8] E. Kawahara, N. Nakada, T. Hikichi, J. Kobayashi, I. Nakanishi, Exp. Cell Res. 272 (2002) 84.
[9] J.T. Price, T. Tiganis, A. Agarwal, D. Djakiew, E.W. Thompson, Cancer Res. 59 (1999) 5475.
[10] L. Soon, G. Mouneimne, J. Segall, J. Wyckoff, J. Condeelis, Cell Motil. Cytoskelet. 62 (2005) 27.
[11] S.J. Wang, W. Saadi, F. Lin, C.M.C. Nguyen, N.L. Jeon, Exp. Cell Res. 300 (2004) 180.
[12] Y. Ito, Biomaterials 20 (1999) 2333–2342.
[13] G.P. Chen, Y.Y. Ito, Biomaterials 22 (2001) 2453.
[14] Y. Ito, Mater. Sci. Eng., C 6 (1998) 267.
[15] C.B. Herbert, T.L. McLernon, C.L. Hypolite, D.N. Adams, L. Pikus, C.C. Huang, G.B. Fields, P.C. Letourneau, M.D. Distefano, W.S. Hu, Chem. Biol. 4 (1997) 731.
[16] B. Liedberg, P. Tengvall, Langmuir 11 (1995) 3821.
[17] B. Liedberg, M. Wirde, Y.T. Tao, P. Tengvall, U. Gelius, Langmuir 13 (1997) 5329.
[18] C.L. Hypolite, T.L. McLernon, D.N. Adams, K.E. Chapman, C.B. Herbert, C.C. Huang, M.D. Distefano, W.S. Hu, Bioconjug. Chem. 8 (1997) 658.
[19] N.L. Jeon, S.K.W. Dertinger, D.T. Chiu, I.S. Choi, A.D. Stroock, G.M. Whitesides, Langmuir 16 (2000) 8311.
[20] S.K.W. Dertinger, X.Y. Jiang, Z.Y. Li, V.N. Murthy, G.M. Whitesides, Proc. Natl. Acad. Sci. U. S. A. 99 (2002) 12542.
[21] R.H. Terrill, K.M. Balss, Y.M. Zhang, P.W. Bohn, J. Am. Chem. Soc. 122 (2000) 988.
[22] K.M. Balss, B.D. Coleman, C.H. Lansford, R.T. Haasch, P.W. Bohn, J. Phys. Chem., B 105 (2001) 8970.
[23] K.M. Balss, G.A. Fried, P.W. Bohn, J. Electrochem. Soc. 149 (2002) C450.
[24] S.T. Plummer, P.W. Bohn, Langmuir 18 (2002) 4142.
[25] K.M. Balss, T.C.B. Kuo, P.W., J. Phys. Chem., B 107 (2003) 994.
[26] C.A. Widrig, C. Chung, M.D. Porter, J. Electroanal. Chem. 310 (1991) 335.
[27] M.M. Walczak, D.D. Popenoe, R.S. Deinhammer, B.D. Lamp, C.K. Chung, M.D. Porter, Langmuir 7 (1991) 2687.
[28] D.E. Weisshaar, B.D. Lamp, M.D. Porter, J. Am. Chem. Soc. 114 (1992) 5860.
[29] D. Hobara, O. Miyake, S. Imabayashi, K. Niki, T. Kakiuchi, Langmuir 14 (1998) 3590.
[30] Q. Wang, P.W. Bohn, J. Phys. Chem., B 107 (2003) 12578.
[31] Q. Wang, J.A. Jakubowski, J.V. Sweedler, P.W. Bohn, Anal. Chem. 76 (2004) 1.
[32] S.T. Plummer, Q. Wang, P.W. Bohn, R. Stockton, M.A. Schwartz, Langmuir 19 (2003) 7528.
[33] D.Q. Xiao, H. Zhang, M. Wirth, Langmuir 18 (2002) 9971.
[34] A. Revzin, R.G. Tompkins, M. Toner, Langmuir 19 (2003) 9855.
[35] K. Mougin, M.B. Lawrence, E.J. Fernandez, A.C. Hillier, Langmuir 20 (2004) 4302.
[36] I. Pockrand, Surf. Sci. 71 (1978) 577.
[37] J.G. Gordon II, II SPIE 276 (1981) 96.
[38] J. Giergiel, C.E. Reed, S. Ushioda, J.C. Hemminger, Phys. Rev., B 31 (1985) 3323.
[39] B.P. Nelson, A.G. Frutos, J.M. Brockman, R.M. Corn, Anal. Chem. 71 (1999) 3928.
[40] A.G. Frutos, J.M. Brockman, R.M. Corn, Langmuir 16 (2000) 2192.
[41] J. Lahiri, L. Isaacs, J. Tien, G.M. Whitesides, Anal. Chem. 71 (1999) 777.
[42] C.D. Tidwell, D.G. Castner, S.L. Golledge, B.D. Ratner, K. Meyer, B. Hagenhoff, A. Benninghoven, Surf. Interface Anal. 31 (2001) 724.
[43] D.Y. Petrovykh, H. Kimura-Suda, M.J. Tarlov, L.J. Whitman, Langmuir 20 (2004) 429.
[44] Y.F. Dufrene, T.G. Marchal, P.G. Rouxhet, Appl. Surf. Sci. 145 (1999) 638.